IMMERSED BOUNDARY METHOD FOR THE ANALYSIS OF 2D FLOW OVER A CYLINDER AND 3D FLOW OVER A SPHERE

D.V. Fernandes,[*1] Y.K. Suh[2] and S. Kang[3]

원통 주위의 2차원 유동과 구 주위의 3차원 유동해석을 위한가상경계법 개발

페르난데스,[*1] 서 용 권,[2] 강 상 모[3]

IB (immersed boundary) method is one of the prominent tool in computational fluid dynamics for the analysis of flows over complex geometries. The IB technique simplyfies the solution procedure by eliminating the requirement of complex body fitted grids and it is also superior in terms of memory requirement. In this study we have developed numerical code (FOTRAN) for the analysis of 2D flow over a cylinder using IB technique. The code is validated by comparing the wake lengths and separation angles given by Guo et. al. We employed fractional-step procedure for solving the Navier-Stokes equations governing the flow and discrete forcing IB technique for imposing boundary conditions. Also we have developed a 3D code for the backward-facing-step flow and flow over a sphere. The reattachment length in backward-facing-step flow was compared with the one given by Nie and Armaly, which has proven the validity of our code.

Key Words : Immersed boundary method, Flow around a cylinder, Flow over a sphere

1. INTRODUCTION

Numericaly solving flow problems involving complex boundaries is one of the great difficulty faced in computational fluid dynamics. The literature shows that a vast number of problems with complex geometries were studied using unstructured body fitted grids. In 1972, Peskin[2] showed that these problems can be numerically studied using a regular orthogonal grid system (cartesian or cylindrical) and later this method was termed as Immersed Boundary(IB) method. The method became popular due to its many advantages over conventional body conformal grids. Such as the task of grid generation is simplified, as IB method uses conventional orthogonal grid. The IB technique is also superior to conventional body conformal grids with respect to memory requirement and CPU-time saving. And even moving boundaries can be easily handled using IBwithout regenerating the grids. But imposing boundary conditions is not straight forward in IB method and also the ramification of boundary treatment will affect the accuracy and conservation properties of numerical scheme.

At present we can see numerous works done in the field of IB method. A brief review of the works done in this field is given here. As mentioned in previous paragraph, C. Peskin introduced this technique first. Afterwards Mohd-Yusof[3] developed a new momentum forcing approach, different from traditional feedback forcing. He applied momentum forcing discretely on the boundary or inside the body. Later Fadlun et al.[4] used this concept to the three dimensinal flow problems with a modification that the forcing is applied in the fluid region near the boundary rather than in the solid. That is, the velocity at the first grid external to the body was obtained by a linear interpolation of velocities at neighbouring grids in fluid region.

Later Kim et al[5]. used the same forcing approach

1 학생회원, 동아대학교 대학원 기계공학과
2 정회원, 동아대학교 기계공학과 교수
3 정회원, 동아대학교 기계공학과 교수
* Corresponding author, E-mail: dolfredf@rediffmail.com

proposed by Mohd-Yusof[3] and additional mass source/sink was applied to the boundary cells to satisfy the mass conservation. Recently, Wei-xi Huang[6] derived a more accurate formulation of the mass source/sink for the virtual cells in fluid crossed by an immersed boundary.

Mittal and Iaccarino[8] reviewed different forcing approaches used in IB method under two broad categories. One is continuous forcing approach where forcing was applied throughout the domain. The other is discrete forcing approach whereforcing applied to the virtual cells cut by an immersed boundary.

In the present study the "discrete forcing approach" is used to impose boundary conditions. The momentum forcing values are obtained by using the procedure given by Kim et al.[5]. The Navier Stokes equations governing the laminar viscous flow are solved using the fractional step method. The following section gives brief description of the method, which is followed by results and discussions section. We compare our results with bench mark problems to confirm the validity of our code.

2. METHODOLOGY

We considered full Navierequations assuming the fluid is incompressible viscous and having constant properties. Luckily the governing equations are independent of the complexity of the geometry, the geometric complexity comes into picture while imposing the boundary conditions. The continuity and momentum equations in non-dimensional form are given below.

$$\frac{\partial u_i}{\partial x_i} = q \tag{1}$$

$$\frac{\partial u_i}{\partial t} + u_j \frac{\partial u_i}{\partial x_j} = \frac{-\partial P}{\partial x_i} + \frac{1}{\mathrm{Re}}\left(\frac{\partial^2 u_i}{\partial x_j^2}\right) + f_i \tag{2}$$

In the above equation f_i's are the momentum forcing components applied to the cell faces near the immersed boundary. q is the mass source/sink applied to the cells containing immersed boundary to satisfy the mass conservation.

We used well known fractional step method for solving the governing equations. The four step procedure is described below. Apseudo-pressure is used to correct the velocity field, so that the continuity equation is satisfied at each computational step. A second order, alternative-direction-implicit (ADI) time advancement scheme is used for time integration. The governing equations are discretized using a 3rd order Runge-Kutta method (RK3) for convection terms and a 2nd order Crank-Nicolson method for the diffusion terms.

Step 1:

$$\frac{\hat{u}_i^k - u_i^{k-1}}{\Delta t} = \alpha_k \left(L(\hat{u}_i^k) + L(u_i^{k-1})\right) - 2\alpha_k \nabla P_i^k - \gamma_k N(u_i^{k-1}) - \rho_k N(u_i^{k-2}) + f_i^k \tag{3}$$

Step 2:

$$\nabla^2 \phi^k = \frac{1}{2\alpha_k \Delta t}\left(\nabla \hat{u}^k - q^k\right) \tag{4}$$

Step 3:

$$u_i^k = \hat{u}_i^k - 2\alpha_k \Delta t \nabla \phi^k \tag{5}$$

$$P^k = P^{k-1} + \phi^k - \frac{\alpha_k \Delta t}{\mathrm{Re}} \nabla^2 \phi^k \quad \text{Step 4:} \tag{6}$$

Where α_k, γ_k and ρ_k are the coefficients of the third order Runge-Kutta method (RK3) and $L(u_i)$and $N(u_i)$ are the linear (diffusion) and non-linear (convection) terms, written in the index notation as follows.

$$L(u_i) = \frac{1}{\mathrm{Re}} \frac{\partial^2 u_i}{\partial x_j \partial x_j} \tag{7}$$

$$N(u_i) = u_j \frac{\partial u_i}{\partial x_j} \tag{8}$$

The intermediate velocity $\hat{u}$ is obtained in step1, and it is corrected in step 3, using the pseudo-pressure ϕ obtained in the step 2. The momentum forcing f_i^k in discrete forcing approach is determined by balancing the discretization equations after imposing the desired velocities in the inertial term. That is if we want to obtain velocity U_i^k at a particular grid point then the momentum forcing f_i^k at that point is;

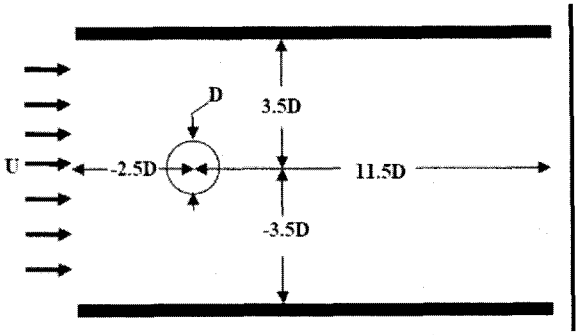

Fig. 1 Schematic of physical domain

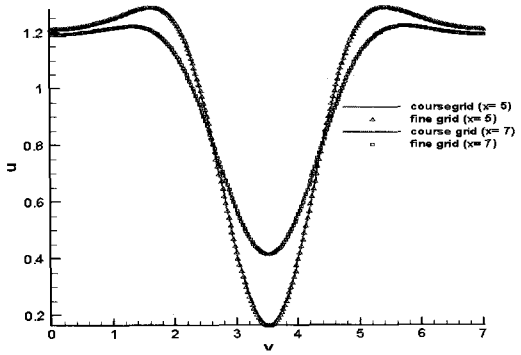

Fig. 2 Grid convergence test for the flow around a cylinder

$$f_i^k = \frac{U_i^k - u_i^{k-1}}{\Delta t} - 2\alpha_k L(u_i^{k-1}) + 2\alpha_k \nabla P_i^k + \gamma_k N(u_i^{k-1}) + \rho_k N(u_i^{k-2}) \quad (9)$$

Where U_i^k is obtained from the explicitly obtained velocities in the fluid region, by interpolation. Either linear or bilinear interpolation is applied based on position of the forcing point with respect to boundary. The mass source/sink q^k in equation (4) is obtained for the cells crossed by the immersed boundary using intermediate velocity components so that continuity is satisfied for these virtual cells. Refer to Kim et al.5] for more general description.

3. RESULTS AND DISCUSSIONS

3.1 FLOW AROUND A CIRCULAR CYLINDER

First we analysed two dimensional flow around a circular cylinder. The domain details are as shown in the Figure 1. The cylinder was placed at the vertical center of channel with cylinder center is 2.5D from the inlet of the channel. The channel is 14D along axial direction, 7D along vertical direction, where D is the diameter of the cylinder. The boundary conditions are as follows;

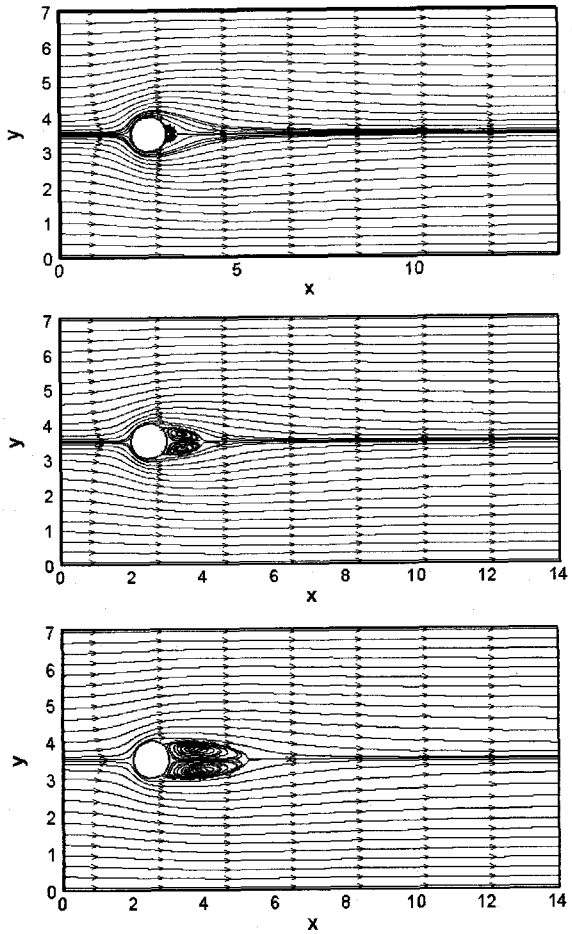

Fig. 3 Streamlines of the steady flow around a circular cylinder for different Reynolds numbers

Inlet $u = U,\ v = 0$

Outlet $\frac{\partial u}{\partial x} = \frac{\partial u}{\partial y} = 0$

Top and bottom walls $\frac{\partial u}{\partial y} = 0,\ v = 0$

Surface of cylinder $u = v = 0$

The Reynolds number ($\mathrm{Re} = DU/\nu$) of the flow is based on the uniform inlet velocity U and the cylinder diameter D. The numerical simulations are carried out for low Reynolds numbers, Re=10, 20 and 40. Also we obtained steady periodic flow at Reynolds number 83.

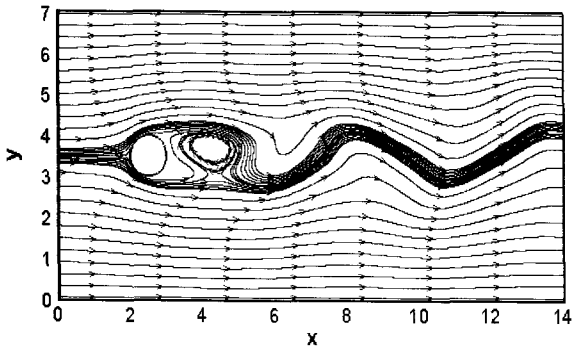

Fig. 4 Instantaneous streamlines of the flow around a circular cylinder for Re=83

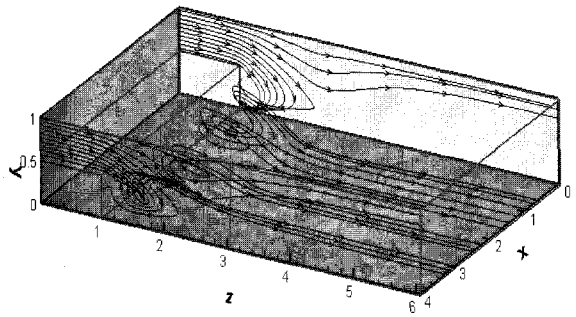

Fig. 5 Streamlines starting from the spanwise planes x=0.05 and x=3.95

We compared ournumerical results obtained using unifrom grid 141 x 281 with those obtained from uniform fine grid 281 x 561, the comparison is shown in the Figure 2. Since there is no significant improvement in the resultsobtained using fine grid we selected 141 x 281 grid for the analysis.

Figure 3 shows the steady state streamlines for

Table 1 Comparison of wake length and reattachment lengths for flow around a cylinder

Researcher's Name	Re					
	10		20		40	
	2Lw/D	Θ	2Lw/D	Θ	2Lw/D	Θ
Nieuwstadt & Keller	0.434	27.96	1.786	43.37	4.357	53.34
Coutanceau & Bouard	0.68	32.5	1.86	44.8	4.26	53.34
He and Doolen	0.474	26.89	1.842	42.9	4.490	52.84
Mei and Shyy	0.498	30.0	1.804	42.1	4.38	50.12
Guo et. al.	0.533	31.61	1.867	42.27	4.4	53.13
Present	**0.58**	**31.7**	**1.87**	**42.4**	**4.4**	**53.08**

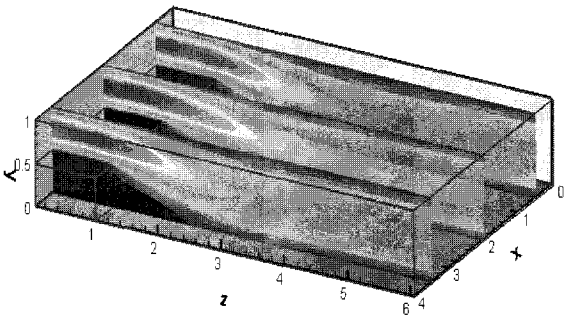

Fig. 6 Axial velocity contours in planes x=0.5, 2.0 and 3.5

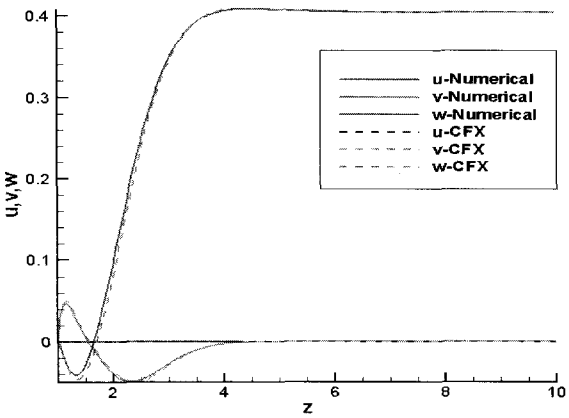

Fig. 7 Comparison of velocities obtained numerically with that obtained using CFX, along a horizontal line at x=2.0 and y=0.25

Reynolds numbers 10, 20 and 40. In all cases a pair of stationary recirculating vortexes found behind the cylinder which grow bigger with the reynolds number. The wake length L_w, the distance from rearmost point of the cylinder to the end of the wake and the separation angle, Θ, are measured. A comparison of present set of data with previous computational and experimental data is given in Table 1. Both the wake length and the separation angle agree well with the results of previous studies for all Reynolds numbers.

Figure 4. shows the instantaneous streamlines during steady periodic flow at Reynolds number 83. This periodic vortex flow was observed after sufficient number of iterations (nondimensional time of 130).

3.2 BACKWARD-FACING-STEP FLOW

We extended our numerical analysis for three dimensional flow cases like "backward-facing-step flow" and "flow over a sphere". The bench mark problem "backward-facing-step flow" is used for validating the

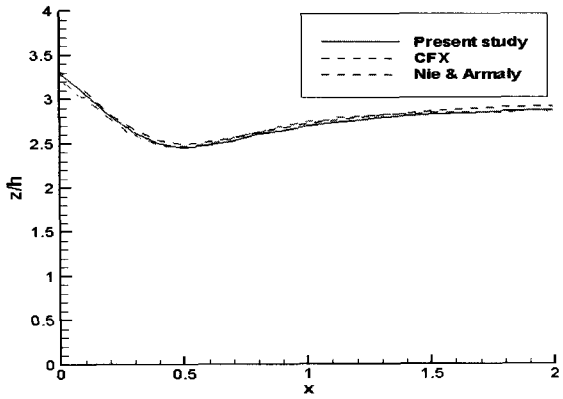

Fig. 8 Lines comprising of the reattachment points along the spanwise direction

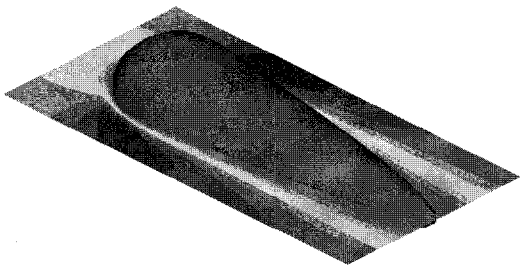

Fig. 9 Iso-surface plot of flow over a sphere for Reynolds number 100

present 3D numerical code. A duct with an inlet aspect ratio a=W/h=8 is taken in order to compare the results given by Nie and Armaly[15]. Here the step hieght h=H/2, that will provide an expansion ratio of 2. The duct length is taken as 10H and the step is located at $0 \leq z \geq 1$. The initial distribution of axial velocity (w) at inlet is the one given by Shah and London[1], while the other velocity components are set equal to zero.At the exit we defined convective boundary conditons and no-slip conditions are applied on the walls.The results obtained using a regular grid of 80x41x201 for Reynolds number 100 are given below. Figure 5, shows some streamlines starting from the spanwise planes x=0.05 and 3.95, indicating there is a recirculation zone downstream of the step. Figure 6. shows axial velocity contours in different planes along the duct.

Also we used commercial code CFX to solve this problem with the same dimensions. The comaparison of velocities obtained from numerical simulation and from CFX simulation is given in Figure 7. The validity of applying convective boundary condition at exit of the duct can be seen in Figure 7, as the flow attains the steady fully developed state at the exit of the duct.

The comparison of reattachment lengths obtained in numerical computation, using comercial code CFX and those given by Nie and Armaly[15] is shown in Figure 8. The reattachment length is the distance from the step to the point where the normal-gradient of the streamwise velocity is zero. In the Figure we have shown the rettachment lengths for the half of the spanwise direction as it is symmetric about the center line.

3.3 FLOW OVER A SPHERE

As an another example of three-dimensional flow, laminar flow over a sphere is simulated for Reynolds numbers 10 and 100. A steady axisymmetric flow is observed for both Reynolds numbers. The computational domain used is 8D in axial direction and 4D in lateral directions, with the sphere centre located at the centre of cross-section at a distance 2.5D from the inlet, where D is diameter of sphere. We have considered smaller domain in order to reduce the computational effort and memory requirements. The boundary conditions are extension of those applied for the flow around the cylinder. Figure 9. shows the iso-surface with contours plot of axisymmetric flow for Reynolds number 100.

4. CONCLUSIONS

We developed numerical codes for 2D flow around a cylinder and 3D flow over a sphere using frctional-step procedure for solving Navier-stokes equations and IB method for imposing boundary conditions. The wake length and the separation angles obtained in our computations were compared with previous results, shows good agreements. For the 3D case we compared the reattachment lengths obtained from our numerical computations, with those obtained from CFX and previous research works. The comparison was excellent. Also we compared the velocities in different positions in the duct with CFX results. All the comparisons were satisfactory, showing the reliabilty of our numerical code.

ACKNOWLEDGEMENTS

This study was supported by the Korea Science and Engineering Foundation (KOSEF) through the National Research Laboratory program funded by the Ministry of Science and Technology (No. 2005-01091).

REFERENCES

[1] 1978, Shah, R.K. and London, A.L., "Laminar Forced Convection in Ducts," *Academic press, New York.*

[2] 1972, Peskin, C.S., "Flow Patterns around heart valves: a digital computer method for solving the equations of motion," *PhD thesis, Physiol., Albert Einstein coll. Med., Uni. Microfilms.*

[3] 1997, Mohd-Yusof, J., "Combined Immersed-Boundary /B-Spline Methods for Simulation of Flow in Complex Geometries," *Annual Research Briefs, Center for Turbulence Research, NASA Ames and Stanford University*, pp.317-327.

[4] 2000, Fadlun, E.A., Verzicco, R., Orlandi, P. and Mohd- Yusof, J., "Combined Immersed Boundary Finite Difference Methods for Three Dimensional Complex Flow Simulations," *J. Comput. Physics* 161, pp.35-60.

[5] 2001, J. Kim., D. Kim. and H. Choi., "An Immersed-Boundary Finite-Volume Method for Simulations of Flow in Complex Geometries," *J. Comput. Physics* 171, pp.132-150.

[6] 2007, Wei-Xi, Huang. and H.J. Sung., "Improvement of Mass Source/Sink for an Immersed Boundary Method, " *Int. J. Numer. Meth. Fluids* 53, pp.1659-1671.

[7] 2004, J. Kim. and H. Choi., "An Immersed-Boundary Finite-Volume Method for Simulations of Heat Transfer in Complex Geometries," *KSME Int.* J.18, pp. 1026-1035.

[8] 2005, Mittal, R. and Iaccarino, G. "Immersed Boundary Method," *Annu Rev. Fluid Mech.* 37, pp.239-261.

[9] 2000, Guo, Z., Shi. B. and Wang, N., "Lattice BGK Model for Incompressible Navier-Stokes Equation," *J. Comput. Physics* 165, pp.288-306.

[10] 1999, Ye, T., Mittal, R., Udayakumar, H.S. and Shyy, W., "An Accurate Cartesian Grid Method for Viscous Incompressible Flows with Complex Immersed Boundaries," *J. Comput. Physics* 156, pp.209-240.

[11] 1981, Peskin, C.S., "Fluid Dynamics of Heart Valves: Experimental, Theoretical and Computational Methods," *Annu Rev. Fluid Mech.* 14, pp.235-259.

[12] 1996, Saiki, E.M. and Biringen, S., "Numerical Simulation of a Cylinder in Uniform Flow: Application of a Virtual Boundary Method," *J. Comput. Physics* 123, pp.450-465.

[13] 1997, Gondret, P., Rakotomalala, N., Rabaud, M., Salin, D. and Watzky, P., "Viscous Parallel Flows in Finite Aspect Ratio Hele-Shaw Cell: Analytical and Numerical Results," *Physics of Fluids* 9, pp.1841-1843.

[14] 1993, Goldstein, D., Handler R. and Sirovich, L., "Modeling a No-slip Flow Boundary with an External Flow Field," *J. Comput. Physics* 105, pp.354-366.

[15] 2003, Nie, J.H. and Armaly, B.F., "Reattachment of Three-Dimensional Flow Adjacent to Backward-Facing Step," *Trans. ASME J. Heat Transfer* 125, pp.422-428.